# Sequence-Specific Conjugates of Oligo(2′-O-methylribonucleotides) and Hairpin Oligocarboxamide Minor-Groove Binders: Design, Synthesis, and Binding Studies with Double-Stranded DNA

**ARTICLE** *in* CHEMISTRY & BIODIVERSITY · JULY 2005

Impact Factor: 1.52 · DOI: 10.1002/cbdv.200590071 · Source: PubMed



**7 AUTHORS**, INCLUDING:

Daria Novopashina
Institute of Chemical Biology and Fundame…
**37** PUBLICATIONS **123** CITATIONS
SEE PROFILE

Alexander Sinyakov
Institute of Chemical Biology and Fundame…
**107** PUBLICATIONS **995** CITATIONS
SEE PROFILE

Vladimir Ryabinin
Institute of Chemical Biology and Fundame…
**85** PUBLICATIONS **272** CITATIONS
SEE PROFILE

Alexandre S Boutorine
Muséum National d'Histoire Naturelle
**74** PUBLICATIONS **1,287** CITATIONS
SEE PROFILE

# Sequence-Specific Conjugates of Oligo(2′-*O*-methylribonucleotides) and Hairpin Oligocarboxamide Minor-Groove Binders: Design, Synthesis, and Binding Studies with Double-Stranded DNA

by **Darya S. Novopashina**[a]), **Alexandre N. Sinyakov**[b]), **Vladimir A. Ryabinin**[b]), **Alya G. Venyaminova**[a]), **Ludovic Halby**[c]), **Jian-Sheng Sun**[c]), and **Alexandre S. Boutorine***[c])

[a]) Institute of Chemical Biology and Fundamental Medicine, Siberian Branch, Russian Academy of Sciences, pr. Lavrentieva 8, 630090 Novosibirsk, Russia (e-mail: danov@niboch.nsc.ru)

[b]) State Research Center of Virology and Biotechnology 'Vector', 630559 Kol'tsovo, Novosibirsk region, Russia (e-mail: sinyakov@niboch.nsc.ru)

[c]) USM 0503 Régulation et Dynamique des Genomes, Muséum National d' Histoire Naturelle, INSERM U565 – CNRS URA 5153, F-75231 Paris Cedex, France (phone: +33-140-79-36-96; fax: +33-140-79-37-05; e-mail: alexandre.boutorine@mnhn.fr)

New conjugates of triplex-forming pyrimidine oligo(2′-*O*-methylribonucleotides) with one or two 'head-to-head' hairpin oligo(*N*-methylpyrrole carboxamide) minor-groove binders (MGBs) attached to the terminal phosphate of the oligonucleotides with a oligo(ethylene glycol) linker were synthesized. It was demonstrated that, under appropriate conditions, the conjugates form stable complexes with double-stranded DNA (dsDNA) similarly to triplex-forming oligo(deoxyribonucleotide) (TFO) conjugates containing 5-methylated cytosines. Kinetic and thermodynamic parameters of the complex formation were evaluated by gel-shift assay and thermal denaturation. Higher melting temperatures ($T_m$), faster complex formation, and lower dissociation constants ($K_d$) of the triple helices (6–7 nM) were observed for complexes of MGB-oligo(2′-*O*-methylribonucleotide) conjugates with the target dsDNA compared to the nonconjugated individual components. Interaction of MGB moieties with the HIV proviral DNA fragment was indicated by UV/VIS absorption changes at 320 nm in the melting curves. The introduction of thymidine *via* a 3′,3′-type 'inverted' phosphodiester linkage at the 3′-end of oligo(2′-*O*-methylribonucleotide) conjugates (3′-protection) had no strong influence on triplex formation, but slightly affected complex stability. At pH 6.0, when one or two hairpin MGBs were attached to the oligonucleotide, both triplex formation and minor-groove binding played important roles in complex formation. When two 'head-to-head' oligo(*N*-methylpyrrole) ligands were attached to the same terminal phosphate of the oligonucleotide or the linker, binding was observed at pH $>7.5$ and at high temperatures (up to 74°). However, under these conditions, binding was retained only by the MGB part of the conjugate.

**1. Introduction.** – Molecules specifically interacting with double-stranded DNA (dsDNA) attract considerable interest because of their possible applications as biologically active compounds capable of acting on genomic DNA. A wide variety of *in vitro* and *in vivo* applications such as site-specific cleavage of DNA [1], mapping of genomic DNA, and selective regulation of gene expression could be envisaged [2][3]. Besides natural, specific peptides, two classes of synthetic molecules are known that recognize and bind specifically to double-stranded DNA sequences: triple-helix-forming oligonucleotides (TFOs) [4–6] and oligo(*N*-methylpyrrole)- and oligo(*N*-methylimidazole) carboxamides as minor-groove binders (MGBs) [7][8].

However, these two classes of sequence-specific agents have certain drawbacks. Oligocarboxamide MGBs with hairpin structures (two oligocarboxamide blocks

separated by a flexible linker) [9][10] recognize quite short DNA sequences according to a discovered code [7][11][12], and need insertion of nonspecific amino acids for their structural adaptation to the DNA minor groove [13]. Triplex-forming oligonucleotides recognize longer sequences, but specifically interact only with polypurine/polypyrimidine dsDNA fragments. Protonation of cytosine in the third strand (facilitated by methylation of cytosine at C(5)) is necessary for *Hoogsteen* H-bond formation; hence, triple helices are stable at slightly acidic pH ($\leq 6.0$). In general, with rare exceptions [14][15], triplexes are not stable under physiological conditions.

To increase the length of the recognized sequence, to stabilize such complexes, and to avoid pH, temperature, and polypurine sequence limitations, covalent linkage of TFOs with MGBs has been proposed [16–18]. The covalent conjugates are able to bind simultaneously to the major and minor grooves of the target DNA in a sequence-specific manner. Stronger and more-specific interaction is provided by two oligocarboxamide strands located in the same DNA minor groove, either in the form of a hairpin [9][10] or two linked, parallel or antiparallel linear oligomers [19–21].

Upon triplex formation, the minor groove of the target DNA duplex is not occupied. We have, thus, compared complex formation by conjugates containing one and two hairpin MGBs attached to the same terminus of the TFO. In our previous publications [20–22], we have demonstrated that, while the attachment of one hairpin MGB to the triplex-forming DNA oligonucleotide increases the stability of the triplex formed without affecting the target duplex stability, the coupling of *two* 'head-to-head' hairpin MGBs to the same oligonucleotide terminus provides considerable effects on the thermal and pH stability on the level of the triple complex and even target DNA duplex formation [17][22].

In the present paper, we studied the kinetics and thermodynamics (equilibrium constants) of triple complex formation under different conditions, and we probed the role of conjugate components and linkers between them in the light of possible mechanisms of interaction. For these studies, we synthesized a series of new conjugates containing TFOs with different modified ribosophosphate backbones (to enhance their resistance to natural endo- and exonucleases) and different linkers between the oligonucleotide and MGB moieties. These conjugates will be more suitable for future *in vivo* tests.

**2. Results.** – 2.1. *Choice of Target, Conjugate Components, and Linkers.* In the choice of a DNA target and conjugate components, we thought both about simpler models and potential biological applications. Thus, a synthetic 29-mer duplex containing a natural polypurine/polypyrimidine sequence of HIV proviral DNA from the genes *nef* and *pol* was chosen as a DNA target [23]. This fragment contains a 16-base-pair (16-bp) polypurine/polypyrimidine sequence and a long 5′-adjacent A/T-tract, thus being a perfectly adapted target for the TFO attached in 5′-position to A/T-specific oligo(*N*-methylpyrrole) carboxamides. The total length of the A/T tract (15 bp), including nine contiguous A/T pairs, one G/C interruption, and again four contiguous A/T pairs, permits for interaction with up to three oligo(*N*-methylpyrrole) carboxamide hairpins comprising six to eight monomers. For practical reasons, we used a duplex of two complementary strands (HIV-D1 and -D2) for the thermal denaturation assay, and a self-complementary oligonucleotide containing these two

strands linked by tetrathymidylate sequence linker (HIV-Loop) for gel-retardation experiments (*Fig. 1*).

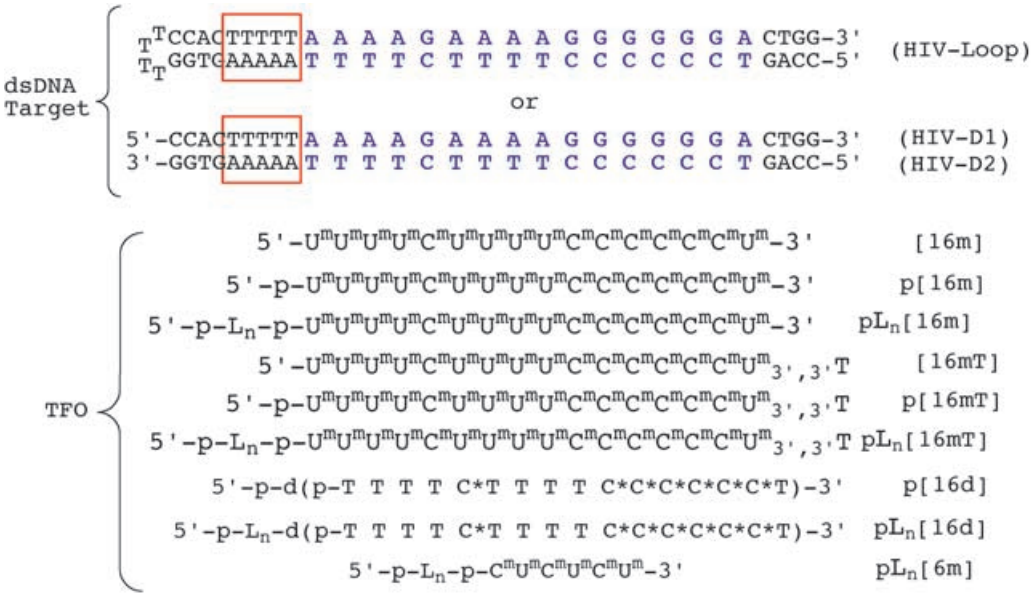


Fig. 1. *Sequences of DNA targets and triplex-forming as well as control oligonucleotides.* Abbreviations: $N^m$ = 2′-*O*-methylribonucleotide; C* = 5-methyldeoxycytidine; $L_n = -(OCH_2CH_2)_n-O-$, $n = 3$ or 6; p = phosphate group. Blue colors indicate the polypurine tract for targeting by TFO. The sequences for MGB interactions are marked by rectangles.

We used oligo(2′-*O*-methylribonucleotides) that not only form quite stable triple helices with target DNA [24–27], but are also accessible by simple synthetic procedures, and exhibit high stability toward endonuclease degradation. To impart the resistance against 3′-exonucleases, a 3′-terminal thymidine was introduced into triplex-forming oligo(2′-*O*-methylribonucleotides) *via* a 3′,3′-phosphodiester linkage (so-called 'inverted' thymidine) [28][29]. Besides enhanced nuclease resistance and easy, inexpensive synthesis, the use of oligo(2′-*O*-methylribonucleotides) permits one to avoid such drawbacks as the toxicity of phosphorothioates and -amidates, non-specific activity, and the presence of diastereoisomers.

As shown earlier, a linker containing at least twelve interatomic bonds has to be introduced between an oligonucleotide and an MGB to enable both components to interact simultaneously in two different DNA grooves [16][17]. Oligo(ethylene glycol) is an advantageous linker because of its hydrophilicity and flexibility. We, thus, used tri- and hexa(ethylene glycol) phosphate linkers for the conjugation of MGBs to oligonucleotides. Different versions of oligonucleotides and linkers (see *Fig. 1*) were used in our studies to elucidate the role of oligonucleotide backbone, terminal phosphate, 3′-protection, and linker length in complex formation efficacy.

2.2. *Oligonucleotide Synthesis.* The solid-phase H-phosphonate method [30] was adapted to the synthesis of oligo(2′-*O*-methylribonucleotides) bearing tri- and hexa-(ethylene glycol) phosphate linkers at the 5′-termini. For this purpose, dimethoxytrityl

(DMT)-protected oligo(ethylene glycol) H-phosphonates were synthesized. Usage of these H-phosphonates at the final step of the synthesis, followed by coupling with '2-[2-(4,4′-dimethoxytrityloxy)ethylsulfonyl]ethanol H-phosphonate' resulted in oligo(2′-*O*-methylribonucleotides) tethered to 5′-oligo(ethylene glycol) phosphate. A series of pyrimidine oligo(2′-*O*-methylribonucleotides) with different linker lengths at the 5′-terminus, their '3′-inverted' analogues stable in biological medium, as well as their DNA versions were synthesized by this method (*Fig. 1*). In DNA versions, all cytosines were 5-methylated to stabilize the protonated form of this base necessary for *Hoogsteen* H-bond formation.

2.3. *Interaction of Target Duplex DNA with Oligo(2′-*O*-methylribonucleotides) and Minor-Groove Binders.* The ability of the synthesized deoxyribonucleotides and oligo(2′-*O*-methylribonucleotides) to form triple helices with dsDNA was shown by both gel-shift and thermal-denaturation assays at pH 6.0. All the oligonucleotides revealed one retarded triplex band in gel-shift experiments. In thermal-denaturation experiments, the difference between the melting curves of triplexes for nonprotected, 3′-protected, or DNA oligonucleotides was not significant ($T_m = 22-24°$), independently of the ribosophosphate backbone type and cytosine modification. Duplex melting was always observed at 67°. Two examples of typical thermal-denaturation curves for triplexes of deoxyribo- and (2′-*O*-methylribo)oligonucleotides are shown in *Fig. 2* (red curves *a*).

We also studied the kinetics of triplex formation by oligo(2′-*O*-methylribonucleotides) using a fluorescence method described previously [31]. The process was quite slow and leveled off after 4–5 h of incubation, very similar to the kinetics of triplex formation observed for analogous oligo(deoxyribonucleotides) as the third strands [31][32] (data not shown).

In contrast, the interaction of free hairpin hexa(*N*-methylpyrrole) carboxamide with dsDNA could not be detected by either method. No shift was observed, when labeled duplex migrated in the gel in the presence of this MGB, and no effect of MGB on $T_m$ of the target duplex was noticed. Concerning triple-helix formation, it has been observed that free minor-groove binders of the netropsin type destabilize triple helices [33][34].

2.4. *Synthesis of Conjugates.* For the synthesis of covalent conjugates of oligonucleotides and hairpin hexa(*N*-methylpyrrole) MGB, we used direct coupling of amino-containing MGB residues to the terminal phosphate group of the oligonucleotides or linkers activated by $Ph_3P$, dipyridyl disulfide, and 4-(dimethylamino)pyridine (DMAP) according to published methods [17][35][36]. As shown recently, when the reaction is carried out in organic media with excess of the activating agent, new activation of the terminal phosphoramidate group takes place, and the second ligand residue can be attached [17][20][37]. The resulting structures are shown in *Fig. 3*.

Oligonucleotide conjugates containing one MGB residue were separated from those with two attached 'head-to-head' MGB residues by reverse-phase high-performance liquid chromatography (RP-HPLC), and analyzed by both denaturing gel electrophoresis and UV spectroscopy. The normalized absorption spectra of the conjugates are shown in *Fig. 4*. Each conjugate spectrum represents a superposition of individual-component spectra. The first peak at 260 nm corresponds to the absorption maximum of the oligonucleotide part, and the second one at 320 nm represents the

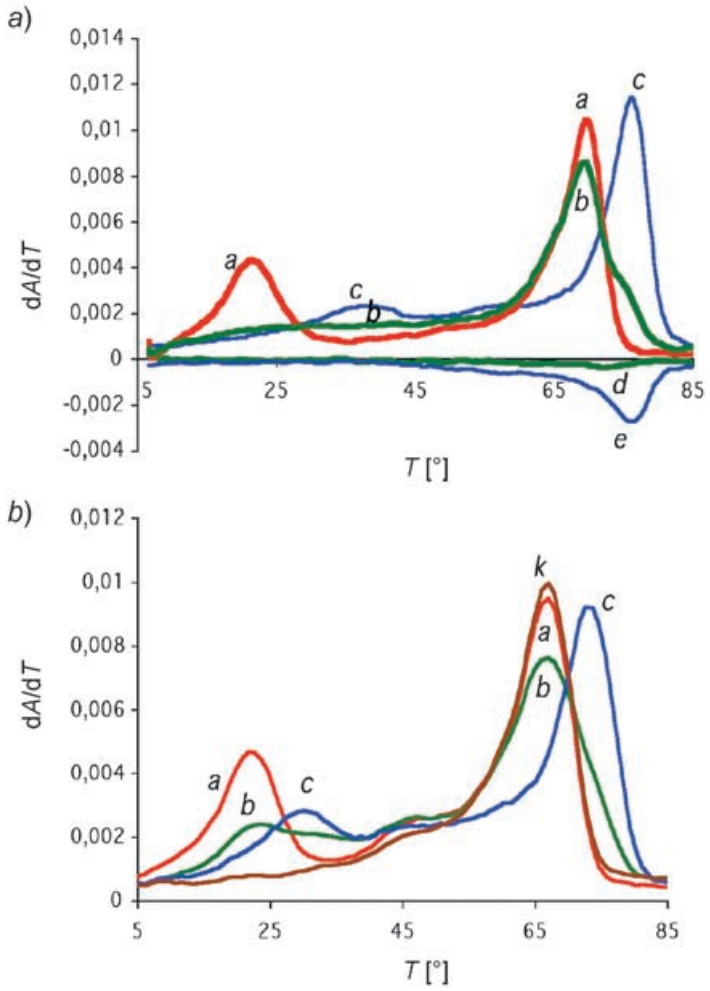


Fig. 2. *First derivatives of the thermal-denaturation curves of the triplexes formed by oligonucleotide conjugates. a*) *Triplexes of the oligo(2′-*O*-methylribonucleotide) conjugates.* Curve *a* (at 260 nm) = p[16mT]; curves *b* (260 nm) and *d* (320 nm) = (MGB)-pL$_6$[16mT]; curves *c* (260 nm) and *e* (320 nm) = (MGB)$_2$-pL$_6$[16m]. *b*) *Triplexes of oligodeoxyribonucleotide conjugates.* Curve *k* (at 260 nm) = control dsDNA target; curve *a* (260 nm) = p[16d]; curve *b* (260 nm) = (MGB)-p*L*$_3$[16d]; curve *c* (260 nm) = (MGB)$_2$-p*L*$_3$[16d]. For melting conditions, see *Exper. Part*.

maximum of the MGB part. For conjugates with one and two MGB residues, respectively, an oligonucleotide/ligand molar ratio of 1:1 and 1:2 was calculated from the molar extinction coefficients of the individual components at these wavelengths. The structures of the conjugates were confirmed by electrospray Q-TOF mass spectrometry (ES-Q-TOF-MS).

2.5. *Complex Formation by Conjugates: Gel-Shift Studies.* We used a gel-shift assay to obtain the thermodynamic and kinetic characteristics of conjugate complex

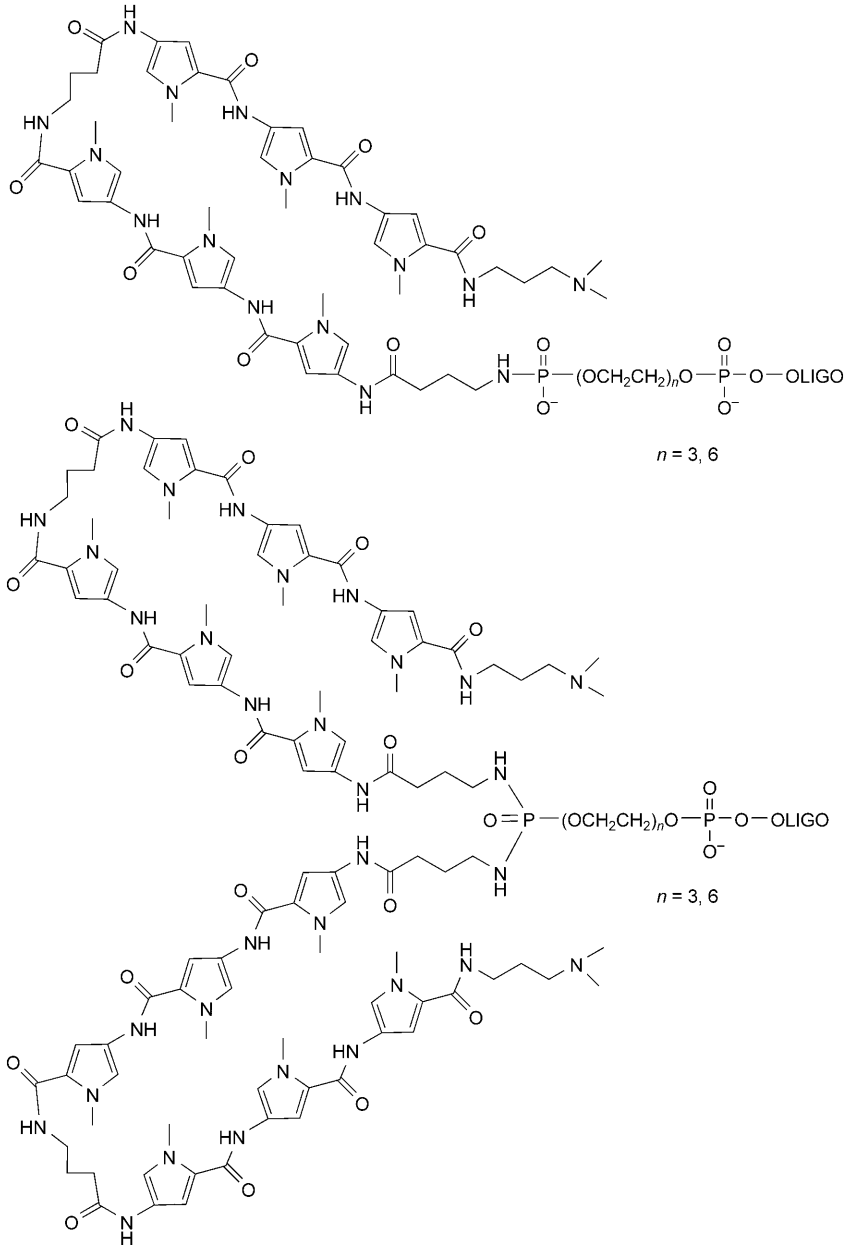


Fig. 3. *Structures of the synthesized oligonucleotide conjugates with one and two hairpin hexa(*N*-methylpyrrole) carboxamide residues.* OLIGO refers to oligonucleotide; $n = 3$ or 6.

formation with the radioactively labeled target DNA duplex. The triple helix was detected, compared to the control duplex band, as a retarded gel-shift band after migration in nondenaturing polyacrylamide gel. Measuring the intensity of this band as

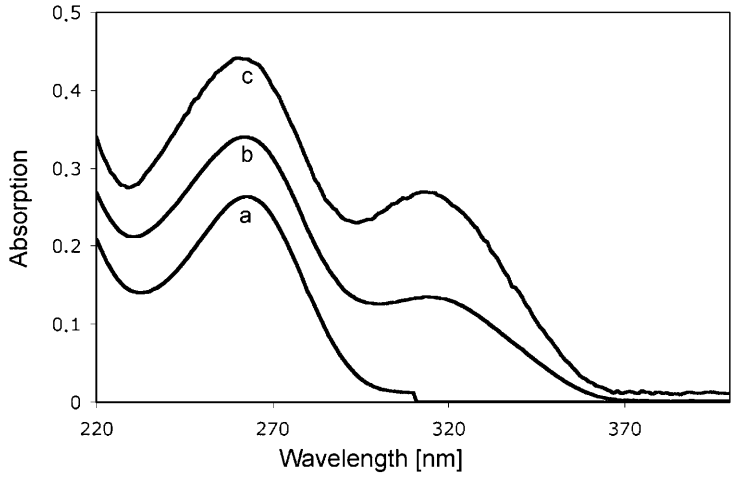


Fig. 4. *Normalized absorption spectra of the initial oligo(2′-*O*-methylribonucleotide) and its conjugates with one or two MGB residues.* Curve $a = pL_3[16m]$; curve $b = (MGB)\text{-}pL_3[16m]$; curve $c = (MGB)_2\text{-}pL_3[16m]$.

a function of incubation time and conjugate concentration allows calculation of triplex-formation rates and complex-dissociation constants. However, it must be noted that gel-electrophoresis separation of the complex does not take place under equilibrium conditions. Thus, gel-shift experiments give only 'apparent' equilibrium or rate constants that are suitable only for comparison of complex-formation processes by different conjugates under identical conditions.

*Fig. 5* shows the gel retardations of the triplexes formed by the oligo(2′-*O*-methylribonucleotide) conjugates with one and two hexa(*N*-methylpyrrole) carboxamide MGB(s) at different pH values. As can be seen from *Fig. 5*, *a*, all the conjugates form triple complexes with the target dsDNA at pH 6.0, independently of the ribosophosphate backbone, absence or presence of one or two attached ligands, and length of the linker in the conjugates (zero, three or six ethylene glycol units). The slight difference in mobility between oligonucleotide alone and its mono- and bis-conjugates was rationalized by their different molecular weights. Overall, the results indicate that the hydrodynamic forms of all the complexes are similar, *i.e.*, in all cases, they migrate as compact triple helices.

A different picture was observed at higher pH values. At pH 7.5 (*Fig. 5*, *b*), no triple-helix formation of oligo(2′-*O*-methylribonucleotide) alone was detected. For oligo(deoxyribonucleotide) containing 5-methylcytosine, a weak, but still notable, retarded band was observed (*Fig. 5*, *b*, lane *2*). This result confirms the previous observation that 5-methylation of cytosine plays an important role in triplex formation at neutral pH, facilitating protonation of cytosines. Attachment of one or two hexa(*N*-methylpyrrole) MGB(s) to the 5′-terminus of oligo(2′-*O*-methylribonucleotide) stimulates triplex formation at pH 7.5 (*Fig. 5*, *b*, lanes *10* and *11*).

In weakly basic medium (pH 8.3), no complex formation between target dsDNA and oligo(2′-*O*-methylribonucleotides), or their conjugates with one MGB residue, was observed, but the conjugates with two MGB residues still formed complexes (*Fig. 5*, *c*,

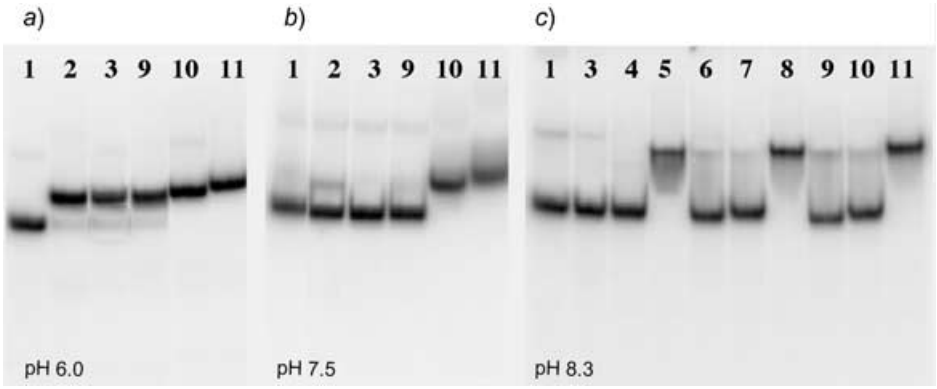


Fig. 5. *Gel-shift analysis of triplex formation by conjugates as a function of pH*. HIV-Loop was used as the target double-stranded DNA. Conditions: at 13° in 12% nondenaturing polyacrylamide gel. *a*) pH 6.0 (buffer: 50 mM *MES*, 50 mM NaCl, 5 mM $MgCl_2$); *b*) pH 7.5 (buffer: 50 mM *HEPES*, 50 mM NaCl, 5 mM $MgCl_2$). *c*) pH 8.3 (buffer: 89 mM *TBE*, 50 mM NaCl, 5 mM $MgCl_2$). Initial dsDNA concentration = 60 nM, concentration of third strand = 10 μM. Lanes: *1* = control dsDNA, *2* = p[16d]; *3* = p[16m], *4* = (MGB)-p[16m], *5* = $(MGB)_2$-p[16m], *6* = $pL_3$[16m], *7* = (MGB)-$pL_3$[16m], *8* = $(MGB)_2$-$pL_3$[16m], *9* = $pL_6$[16m], *10* = (MGB)-$pL_6$[16m], *11* = $(MGB)_2$-$pL_6$[16m].

lanes *5*, *8*, and *11*). It must be noted that, at pH 8.3, the triple complexes migrate much slower than at lower pH (compare lanes *11* in *Fig. 5*), which indicates that there is no more-compact triple helix under more-basic conditions. Apparently, the DNA triple helix is dissociated, and the triple complex is retained only by interactions between bis-conjugates of MGB and dsDNA. A similar, highly retarded band was also observed, when gel electrophoresis of the complex with MGB bis-conjugates was performed at pH 6.0–8.3 at elevated temperatures of up to 65° (data not shown).

The non-cognate oligo(2′-*O*-methylribonucleotide) $C^mT^mC^mT^mC^mT^m$ or the permutated DNA 16-mer TCTCTCTTCCTTCTTC (with 5-methylated cytosines) did not form triple helices with the target dsDNA under various conditions. Their conjugates with one MGB also did not reveal a retarded band in the nondenaturing gel. However, when two MGB molecules were attached to noncognate oligonucleotides, their dsDNA complexes were formed in all pH ranges studied. In *Fig. 6*, the gel-shift assays of noncognate bis-conjugates at different pH are shown. The case of the bis-conjugate of the permutated 16-meric deoxyribonucleotide at pH 6.0 is especially interesting, because it has exactly the same molecular weight as the cognate conjugate. Its complex with the target DNA migrates much slower, though, than that of the cognate one (*Fig. 6*, lanes *2* vs. *3*), similarly to the cognate conjugate at higher pH. Thus, in this case, only the bis-MGB part of the conjugate interacts with the dsDNA target.

2.6. *Comparison of the Apparent Dissociation Constants and Kinetics of Triple-Complex Formation*. Triplex dissociation constants ($K_d$) at a temperature of 13° and at pH 6.0 were calculated from gel-shift experiments for different concentrations of the third strand (*Table 1*). The $K_d$ values for the triplex formed by oligo(2′-*O*-methylribonucleotide) with dsDNA was less than two times higher than that for triplexes formed by the deoxyribo analogue with 5-methylcytosines. A decrease in $K_d$ was observed, when the oligo(ethylene glycol) phosphate linker was attached to the 5′-

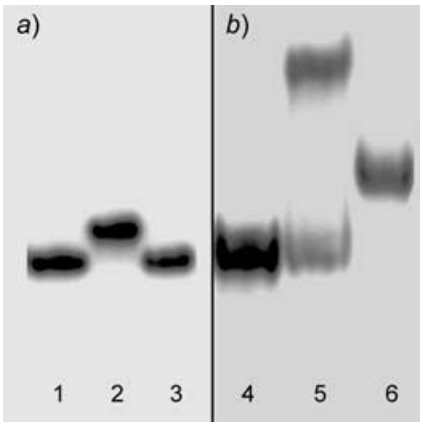


Fig. 6. *Gel-shift analysis of complex formation by conjugates of noncognate oligonucleotides at* a) *pH 8.3* vs. b) *pH 6.0*. For buffers, see legend to *Fig. 5*. HIV-Loop was used as a target double-stranded DNA. In 12% nondenaturing polyacrylamide gel at 13°. Lanes: *1* and *4* = no conjugate, *2* = conjugate $(MGB)_2$-$pL_6$[6m], *3* = conjugate (MGB)-$pL_6$[6m], *5* = conjugate $(MGB)_2$-$pL_6$[TC*TC*TC*TTC*C*TTC*TTC*]; *6* = conjugate $(MGB)_2$-$pL_6$[16d].

Table 1. *Apparent Triplex Dissociation Constants of Complexes between Double-Stranded DNA and Different Conjugates at pH 6.0.* Note, 'p' designates phosphate groups, and 'L' stands for ethylene glycol linker; for compound constitutions, see *Fig. 1*.

| Compound | $K_d$ [nM] | Compound | $K_d$ [nM] |
|---|---|---|---|
| [16d] | 66 ± 12 | $(MGB)_2$-$pL_6$[16m] | 6 ± 3 |
| p[16d] | 92 ± 12 | [16mT] | 149 ± 36 |
| p[16m] | 149 ± 36 | p[16mT] | 308 ± 52 |
| $pL_6$[16m] | 67 ± 1 | $pL_3$[16mT] | 291 ± 35 |
| (MGB)-p[16m] | 68 ± 9 | $pL_6$[16mT] | 187 ± 30 |
| $(MGB)_2$-p[16m] | 63 ± 4 | (MGB)-$pL_6$[16mT] | 84 ± 3 |
| (MGB)-$pL_3$[16m] | 81 ± 6 | $(MGB)_2$-$pL_6$[16mT] | 64 ± 4 |
| $(MGB)_2$-$pL_3$[16m] | 14 ± 7 | $(MGB)_2$-$pL_6$[6m] | 189 ± 28 |
| (MGB)-$pL_6$[16m] | 7 ± 4 | | |

terminus of the oligonucleotide. The reason for this stabilization is not clear; possibly, it has to do with the two negative charges of the terminal phosphate being separated from the triplex by several ethylene glycol units.

Attachment of thymidine *via* a 3′,3′-phosphodiester linkage also destabilized the triple helix. Upon attachment of MGB to 3′-protected oligonucleotide, the same tendency in $K_d$ changes was observed for its conjugates; however, in the case of 3′,3′-type 'inverted' thymidine, all the constants were higher.

When one or two MGB(s) were attached directly to the 5′-phosphate of the oligonucleotide, without any linker, the dissociation constants of the triple complex at pH 6 were the same as for the oligonucleotide comprising just an oligo(ethylene glycol) linker. This means that, at this pH, MGB does not play a crucial role in complex formation, because the distance between the TFO and MGB parts is not long enough to join two components in different grooves. Attachment of one or two MGB molecules to

oligo(2′-*O*-methylribonucleotides) *via* a tri- or hexa(ethylene glycol) phosphate linker decreased the $K_d$ value of the triplex. The strongest effect (up to 20-fold decrease) was observed, when hexa(ethylene glycol) was used as a linker between the oligo(2′-*O*-methylribonucleotides) and the MGB(s).

The contribution of MGB to the interaction with target DNA was revealed in experiments with conjugates of the noncognate oligonucleotide $C^mT^mC^mT^mC^mT^m$. As mentioned above, the MGB bis-conjugate of this oligonucleotide exhibited a retardation gel-shift band with the target (*Fig. 6*). The $K_d$ value for this complex was estimated to be *ca.* 200 nM.

To compare apparent rates of triplex formation by different oligo(2′-*O*-methylribonucleotide) MGB conjugates, we used the so-called 'stop-in-gel' retardation experiments. In time intervals of 15, 30, and 60 min (*etc.*) after mixing of dsDNA with the third strand at different concentrations, the aliquots were charged on the nondenaturing gel, and then immediately submitted to electrophoretic migration. Then, the part of the labeled target DNA in the complex was calculated as a function of incubation time and concentration for each lane, and the data were processed with the SigmaPlot software to derive 'apparent' rate constants $k_1$ (*Table 2*; see also *Exper. Part*). As can be seen, the introduction of MGB residues into the oligo(2′-*O*-methylribonucleotide) increased the association rates of triplex formation considerably: 15 times for the mono-conjugate, and *ca.* 30 times for the bis-conjugate.

Table 2. *Apparent Kinetic Constants of Triplex Formation between Different Conjugates and Double-Stranded DNA at pH 6.0*

| Oligomer | $k_1 \times 10^{-2}$ [$M^{-1}$ $s^{-1}$] |
|---|---|
| $pL_3$[16m] | $1.1 \pm 0.4$ |
| (MGB)-$pL_3$[16m] | $15 \pm 5$ |
| $(MGB)_2$-$pL_3$[16m] | $27 \pm 10$ |

2.7. *Complex Formation by Conjugates: Thermal-Denaturation Studies.* Typical thermal-denaturation experiments are shown in *Fig. 2*. These results are representative for all the series of synthesized oligonucleotides and conjugates. The first derivatives of melting curves of the oligo(2′-*O*-methylribonucleotide) conjugate complexes with dsDNA were compared with their deoxyribo analogues. The melting curves of control triple helices with nonconjugated oligonucleotides revealed two clear transitions: triplex melting at 24°, and duplex melting at 67°.

Attachment of one or two hexa(*N*-methylpyrrole) MGB(s) to oligo(2′-*O*-methylribonucleotides) changed the character of the thermal denaturation. When one MGB residue at the 5′-end of the nucleotide was introduced, no acute 'triplex → duplex' transition was indicated by the melting curve, indicating low cooperativity of this process (*Fig. 2*, curves *b*). This transition was better expressed for DNA oligonucleotide: as can be seen in *Fig. 2*, *b* (curve *b*), a low and broad peak at 24–28° was found. In fact, in different experiments with mono-substituted conjugates, this peak was not very reproducible and resembled either a mounting line or was broad, with a maximum in the temperature interval between 24 and 35°. No triplex → duplex transition was observed at pH 7.5–8.3. The melting temperature (68°) of the target duplex was not changed, however, the peak indicating duplex melting was broader and had a shoulder

at higher temperature (curves *b*), indicating a possible weak interaction of conjugated MGB with DNA.

When two parallel MGB ligands were attached to the 5′-terminus of the oligonucleotide, the triplex melting at pH 6.0 was more reproducible, being observed in the form of a low and broad melting peak at 30–38° for all bis-conjugates. Most interestingly, the $T_m$ value of the target duplex increased by 6° (from 68 to 74°) in this case. This shift was observed both for oligo(2′-*O*-methylribonucleotides) and for their deoxyribo analogues conjugated with two MGB residues. The increase of the melting temperature of the target duplex, in the presence of the MGB bis-conjugates, was dependent on neither pH nor the length of the linker.

In one of our previous publications [20], we have shown that a decrease in light absorption at 320 nm due to a shift in the absorption maximum during thermal denaturation experiments is a clear indication of the interaction and binding between dsDNA and oligocarboxamide MGBs. On the melting-curve derivatives at 320 nm, this effect is seen as a negative peak, with a minimum in a melting point of the dsDNA–MGB complex. In *Fig. 2*,*a* (curve *e*), this negative peak is observed at 74°, at the melting point of the target double strand. For the 1:1 conjugate or for the free MGB molecule, this effect was hardly observed. So, two 'head-to-head' hairpin MGBs linked to the same terminal phosphate of the oligonucleotide stabilize tertiary complexes, and even target duplexes, due to their strong interaction with dsDNA.

**3. Discussion.** – The first conclusion from the above experiments is that, for the design of anti-gene reagents, triplex-forming deoxyribonucleotides can be replaced by oligo(2′-*O*-methylribonucleotides). While this type of synthetic oligonucleotides do not demonstrate additional kinetic or thermodynamic advantages regarding triplex formation relative to DNA analogues [17] (in this sense, they actually have very similar properties), they are resistant to endoribo- and deoxyribonucleases. Moreover, they are less expensive than LNA, and do not suffer from the known drawbacks associated with modified backbones (phosphorothioates and phosphoramidates). Protection from exonucleases by 3′,3′-inversion of 3′-terminal nucleotides does not affect drastically complex formation, but strongly protects the integrity of oligonucleotides in biological media [28].

In general, conjugates of oligonucleotides with minor groove binders have higher affinity for target dsDNA, and recognize longer DNA sequences than individual components, accelerating triplex formation and stabilizing the complex. Melting temperatures of the triplexes as well as their pH stabilities are affected. The optimal linker to join two recognition moieties is hexa(ethylene glycol) phosphate.

Stabilization of triple complexes by attachment of one hairpin oligocarboxamide has been reported by *Dervan* and co-workers [16]. We have also observed both stimulation and a 15-fold acceleration of triplex formation at pH 7.5, and a decrease in the triplex dissociation constant upon MGB attachment by one order of magnitude (*Tables 1* and *2*). According to the gel-migration rate, at pH 6.0 and 7.5, both components participate in complex formation, and a real triple helix is produced by oligonucleotide and target dsDNA. This observation is very important for the biological applications of the conjugates because it allows for triple-helix formation at physiological pH.

It is not easy to describe the role of oligocarboxamides regarding thermodynamic stability of triplexes, and its interaction with DNA, because no evident cooperative triplex → duplex transition was indicated in the melting-curve experiments. Clearly, the third strand dissociates from the complex at higher pH and temperature. However, the question of residual interaction between the MGB component and the target duplex after third-strand dissociation is not so evident. While the melting curve at 320 nm reveals a negligible negative peak, the duplex melting curve recorded at 260 nm (*Fig. 2*, curves *b* and *d*) is broader and has a shoulder above 67°. This shoulder may reflect a weak interaction between MGB and dsDNA, and a partial stabilization of the duplex by this interaction.

A different situation is observed, when two hairpin minor-groove binders are attached to the same oligonucleotide. First, the rate of complex formation is accelerated *ca.* 30 times compared to oligonucleotide alone, and the dissociation constants of the triple complex decrease by *ca*. one order of magnitude. At pH 6.0 and 7.5, a real triple helix forms, both oligonucleotide and MGB parts contributing to the formation of the complex. According to thermal-denaturation data, the melting point of the triplex formed at pH 6.0 by the oligonucleotide part of this conjugate is 8–14° higher ($T_m = 32–37°$) compared to the nonconjugated oligonucleotide. The melting of the target duplex proceeds at higher temperature (74°), simultaneously with MGB dissociation. At higher pH or upon heating, the complex still exists, but migrates in gel slower than a control triple helix, which indicates a less-compact overall structure. We ascribe this to the oligonucleotide third strand dissociating from the major groove, with only the MGB part of the conjugate interacting with dsDNA. In addition, when the cognate oligonucleotide is replaced with a mutated one, the resulting complex forms, but migrates much more slowly in the gel, even at acidic pH and low temperature.

Thus, our experiments demonstrate a special behavior of two 'head-to-head' MGB moieties attached to the same oligonucleotides. Attachment of two MGB residues is more efficient for both complex formation and stability. In this case, at acidic and neutral pH, TFO serves as an 'address', and directs the conjugate to a specific location, and the minor groove binder accelerates complex formation and strongly stabilizes the complex.

The 'head-to-head' hairpin hexa- or octa(*N*-methylpyrrole) carboxamide constructions could be interesting by themselves for the specific recognition of the long A/T repeats on double-stranded DNA. Use of *N*-methylimidazole and other carboxamides [12] could extend their applications to any dsDNA sequence. In this case, an interesting question of disposition and orientation of this 'bis-MGB' in the dsDNA minor groove arises. In fact, five A/T pairs from the 5′-side of a polypurine tract is not enough to bind six *N*-methylpyrrole pairs in a parallel extended orientation, hence, such a position is not very probable.

Our hypothesis is that, in the complex, the MGB interacts with DNA conserving its hairpin form. When only one MGB is attached to the oligonucleotide, it can insert either into the 5′-adjacent or into the triplex-forming part of the target duplex minor groove. Taking into account previously published data [33][34], we suppose that it is actually the 5′-adjacent part. Interaction of this moiety with DNA is quite weak after dissociation of the oligonucleotide part. When two 'head-to-head' MGB moieties are attached, both of them keep their hairpin conformation, and one is located in the minor

groove of the 5′-adjacent A/T sequence, whereas the second one interacts with a part of a triplex-forming sequence in its minor groove (*Fig. 7*). Due to structural reasons not yet understood, such a complex is not only extremely stable by itself, but also retains together two strands of a target duplex.

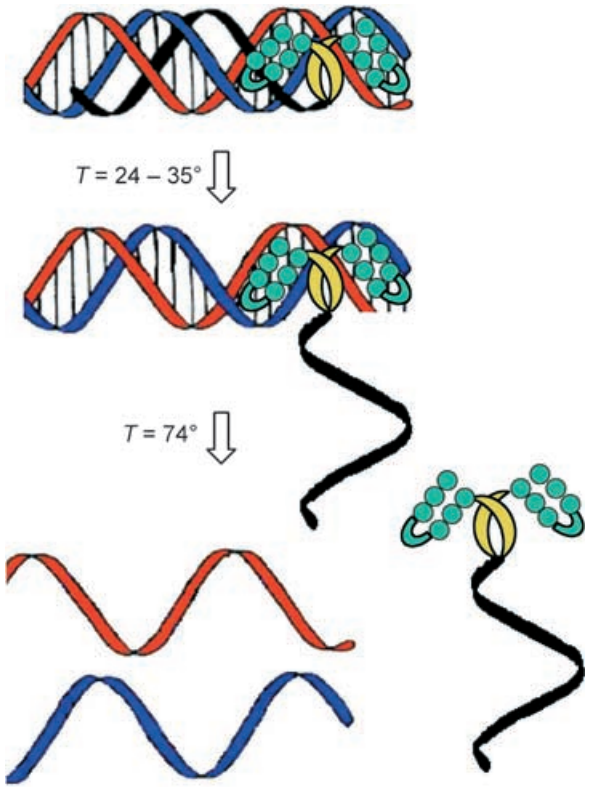


Fig. 7. *Proposed schematic interaction between a double-stranded DNA fragment and a conjugate made of a triple-helix-forming oligonucleotide* (TFO) *and two oligo(*N*-methylpyrrole carboxamide) minor-groove binders* (MGBs)

The constructions proposed in this work could be considered as molecular instruments for the detection of certain sequences (or genes) in double-stranded DNA in biological experiments, and for artificial, sequence-specific regulation of gene expression.

This work was supported by *INSERM*, *CNRS*, the *Muséum National d' Histoire Naturelle*, the *European Commission* (INTAS, project 2001-0638), and the *Ministry of Foreign Affairs of France* (project EGIDE No. 04542ND). We express our acknowledgements to Dr. *J. P. Brouard* and *L. Dubost* for recording mass spectra.

## Experimental Part

*General.* Reagents, sorbents, and solvents were purchased from *Sigma-Aldrich-Fluka*, *VWR International*, and *Reachim* (Russia). 3′-H-Phosphonates of *N*-protected 5′-*O*-dimethoxytrityl-2′-*O*-methylribonucleosides were obtained as described [38]. 3′-*O*-(Dimethoxytrityl)thymidine was synthesized according to [39].

Oligo(deoxyribonucleotides) and their 5-methylcytosine containing analogues were purchased from *Eurogentec* (Belgium). Snake venom phosphodiesterase (EC 3.1.4.1) and *Penicillium citrinum* nuclease P1 (EC 3.1.30.1) were purchased from *Sigma*, *E. coli* alkaline phosphatase (EC 3.1.3.1) was obtained from *Biolar* (Latvia), and T4 polynucleotide kinase (EC 2.7.1.78) was available from *New England BioLabs*. Oligonucleotides and their analogues were purified by anion-exchange HPLC, followed by RP-HPLC on *Waters* instruments. Anal. and quant. RPC analysis was performed with a *Milichrom* (Russia) chromatograph. Anal. and prep. HPLC of MGB and MGB conjugates was performed with an *Agilent-1100* chromatography system. UV/VIS Spectra were recorded on a *Kontron 923 Uvikon* instrument (*Bio-Tek*) in 1-cm quartz cuvettes; $\lambda_{max}$ in nm (log $\varepsilon$). Fluorescence spectra were recorded on a *Spex Fluorolog DM1B* instrument (USA) in $0.2 \times 1$ cm quartz cuvettes. $^{31}$P-NMR Spectra were recorded on a *Bruker AM-400* spectrometer in pyridine/MeCN 1:1 relative to 85% $H_3PO_4$ as an external standard; $\delta$ in ppm, $J$ in Hz. ES-Q-TOF Mass spectra were recorded on a *Q-Star* (*Applied Biosystems*) spectrometer. Radioactive gels were visualized with a *PhosphoroImager* instrument (*Molecular Dynamics*), and the data were analyzed with the ImageQuant software.

*Syntheses of Oligo(2′-*O*-methylribonucleotides)*. Attachment of the first nucleoside moiety to the *CPG-500* solid carrier containing carboxylic acid groups was carried out as described in [40]. The average loading was 35–45 μmol per gram of carrier.

*2-[2-(4,4-Dimethoxytrityloxy)ethylsulfonyl]ethanol H-Phosphonate.* 2-[2-(4,4-Dimethoxytrityloxy)ethylsulfonyl]ethanol was synthesized according to [41] in a yield of 85%, and then transformed in 74% yield into the H-phosphonate similarly as described in [42]. $^{31}$P-NMR: 2.63 ($d$, $J$(P,H) = 607).

O-*(4,4′-Dimethoxytrityl)tri(ethylene glycol) and* O-*(4,4′-Dimethoxytrityl)hexa(ethylene glycol) H-Phosphonates.* Dimethoxytrityl (DMT)-containing derivatives of tri- ($n = 3$) and hexa(ethylene glycol) ($n = 6$) were prepared as described in [43] in yields of 80–85%. The corresponding H-phosphonates were prepared by analogy with a protocol for the synthesis of deoxyribonucleoside H-phosphonates [44] in yields of 50–60%. $^{31}$P-NMR: 4.77 ($d$, $J$(P,H) = 933; for $n = 3$); 4.73 ($d$, $J$(P,H) = 933; for $n = 6$).

*Oligo(2′-*O*-methylribonucleotides)*. The 2′-*O*-Me oligomers were obtained according to a protocol of manual solid-phase H-phosphonate synthesis using a column with a porous filter [30]. The synthesis of 3′-modified oligomers was carried out on polymer support with bound 3′-*O*-(4,4′-dimethoxytrityl)thymidine. Sequential usage of tri- or hexa(ethylene glycol) H-phosphonate and 2-[2-(4,4′-dimethoxytrityloxy)ethylsulfonyl]ethanol H-phosphonate in the two final steps of the synthesis resulted in oligo(2′-*O*-methylribonucleotides) with an oligo(ethylene glycol) phosphate linker at the 5′-end. The compounds were synthesized on a scale of 1–4 μmol (50–100 mg of CPG-bound nucleoside).

*Purification of Oligonucleotides.* After removal of the carrier and the N-protecting groups under standard conditions, the oligonucleotides were purified first by ion-exchange HPLC on a *Polysil SA* column ($4.6 \times$ 250 mm; *Teor. Praktika*, Russia), eluting with a linear gradient of 30% MeCN in aq. $KH_2PO_4$ (0–0.3M, pH 6.5). Further purification was achieved by RP-HPLC on a *Lichrosorb RP-18* column ($4.6 \times 250$ mm; *Merck*, Germany), with a linear gradient of 0–20% MeCN in 50 mM aq. $LiClO_4$ soln. The oligonucleotides were precipitated with 2% $LiClO_4$ in acetone, and washed with acetone to afford the target compounds in 15–21% yield.

*Analysis of Nucleoside Composition.* The nucleoside compositions of the oligo(2′-*O*-methylribonucleotides) were confirmed by exhaustive enzymatic hydrolysis with a mixture of PDE and alkaline phosphatase, or (in the case of 3′,3′-type 'inverted' analogues) with nuclease P1 and alkaline phosphatase under standard conditions. Quant. analysis of the hydrolyzate by anal. RP-HPLC (*Nucleosil C-18* (5 μm), $2 \times 62$ mm; *Macherey-Nagel*, Germany), with a linear gradient of 0–80% MeOH in 50 mM aq. $LiClO_4$ soln. was performed. Retention times ($t_R$)) and spectral ratios were compared with monomer standards. The exper. nucleoside ratios corresponded to the calculated ones.

*Synthesis of Minor-Groove Binders* (MGBs). The synthesis, purification, and characterization (NMR, MS) of amino-functionalized MGBs was carried out as described previously [44–46], with small modifications. Thus, after liquid-phase synthesis, all the products were transformed into the free-amine form, additionally separated from water-soluble impurities by precipitation in 20% aq. $NH_3$ soln., transformed into their trifluoroacetates (TFA salts), and finally purified by semi-prep. HPLC on a *C-18 X-Terra* (7 μm) column ($7.8 \times 300$ mm; *Waters*), using a linear gradient of 0–80% MeCN in $H_2O$ containing 0.1% of TFA at a flow rate of 2 ml/min. After solvent removal, the MGBs were dried *in vacuo*.

*Synthesis of Oligonucleotide–MGB Conjugates.* Conjugates bearing one or two MGB residues at the 5′-end were prepared according to [17]. To a soln. of the oligonucleotide (anh. cetyltrimethylammonium salt; 150–250 μg, 30–50 nmol) in anh. DMSO (50 μl), were added 4-(dimethylamino)pyridine (DMAP; 5 mg, 40 μmol), dipyridyl disulfide (6.6 mg, 30 μmol), and $Ph_3P$ (7.9 mg, 30 μmol) in DMSO (25 μl each). This mixture was

shaken during 20 min. Then, a soln. of the MGB (25 μmol) in DMSO (25 μl) and $Et_3N$ (5 μl) were added, and the mixture was incubated at r.t. for 2 h (or, preferably, overnight), followed by precipitation with 2% $LiClO_4$ soln. in acetone. The precipitate was washed with acetone, dried, and dissolved in $H_2O$. Both the mono- and bis-conjugate(s) were formed in total yields of 70–90%.

*Purification and Analysis of Conjugates.* The conjugate products were purified by HPLC on a *C-18 X-Terra* (7 μm) column (7.8 × 300 mm; *Waters*), using a linear gradient of 5–40% MeCN in 0.02M aq. $NH_4OAc$ soln. (pH 6) at a flow rate of 2 ml/min, and then precipitated as the Na salts from EtOH. The retention times ($t_R$) were 8.3–9.1 min for the starting oligonucleotides, 12–17 min for the oligonucleotide conjugates with one MGB residue (1:1 conjugates), and 15–22 min for the conjugates with two MGB residues (2:1 conjugates). The yields were 35–40% for the 1:1 conjugates, and 25–30% for the 2:1 conjugates. The purities of the conjugates were confirmed by standard 20% denaturing PAGE. Molar extinction coefficients $\varepsilon$ at 260 nm of the oligonucleotide conjugates were calculated from the sum of $\varepsilon$ values of the corresponding unmodified oligonucleotide and those of the MGB (36610 $M^{-1}$ $cm^{-1}$) [47].

*(MGB)-p[16m]*. HPLC: $t_R$ 12.9 min. UV ($H_2O$): 260 (5.24), 320 (4.84). ES-Q-TOF-MS: 6120.74 ($[M-H]^-$; calc. 6121.33).

*$(MGB)_2$-p[16m]*. HPLC: $t_R$ 16.2 min. UV ($H_2O$): 260 (5.33), 320 (5.14). ES-Q-TOF MS: 7108.02 ($[M-H]^-$; calc. 7108.45).

*(MGB)-$pL_3$[16m]*. HPLC: $t_R$ 12.9 min. UV ($H_2O$): 260 (5.24), 320 (4.84). ES-Q-TOF-MS: 6332.77 ($[M-H]^-$; calc. 6333.46).

*$(MGB)_2$-$pL_3$[16m]*. HPLC: $t_R$ 16.1 min. UV ($H_2O$): 260 (5.33), 320 (5.14). ES-Q-TOF-MS: 7319.86 ($[M-H]^-$; calc. 7320.58).

*(MGB)-$pL_6$[16m]*. HPLC: $t_R$ 13.5 min. UV ($H_2O$): 260 (5.24), 320 (4.84). ES-Q-TOF-MS: 6465.57 ($[M-H]^-$; calc. 6465.62).

*$(MGB)_2$-$pL_6$[16m]*. HPLC: $t_R$ 16.5 min. UV ($H_2O$): 260 (5.33), 320 (5.14). ES-Q-TOF-MS: 7452.57 ($[M-H]^-$; calc. 7452.7).

*(MGB)-$pL_6$[16mT]*. HPLC: $t_R$ 13.8 min. UV ($H_2O$): 260 (5.26), 320 (4.84). ES-Q-TOF-MS: 6690.05 ($[M-H]^-$; calc. 6689.8).

*$(MGB)_2$-$pL_6$[16mT]*. HPLC: $t_R$ 16.8 min. UV ($H_2O$): 260 (5.34), 320 (5.14). ES-Q-TOF-MS: 7677.02 ($[M-H]^-$; calc. 7676.95).

*(MGB)-$pL_6$[6m]*. HPLC: $t_R$ 15.4 min. UV ($H_2O$): 260 (4.95), 320 (4.84). ES-Q-TOF-MS: 3382.5 ($[M-H]^-$; calc. 3385.7).

*$(MGB)_2$-$pL_6$[6m]*. HPLC: $t_R$ 18.5 min. UV ($H_2O$): 260 (5.11), 320 (5.14). ES-Q-TOF-MS: 4393.1 ($[M-H]^-$; calc. 4390.9).

*Thermal-Denaturation Assay.* This assay was carried out in 0.01M cacodylate buffer (pH 6.0), 0.1M aq. NaCl soln., and 5 mM aq. $MgCl_2$ soln. The concentrations of the strands in each sample were 1–1.3 μM for the target duplex (HIV-D1 and -D2), and 1.3–1.7 μM for the third strand. The sample temp. was changed in steps of 0.1°/min, and the absorption was recorded every 200 s at 260, 320, and 580 nm.

*Gel-Mobility-Shift Assay.* Gel-shift experiments were performed in 12% nondenaturing polyacrylamide gel by electrophoresis in 50 mM *MES* (pH 6.0), 50 mM aq. NaCl soln., and 5 mM aq. $MgCl_2$ soln. Each sample (8–10 μl) contained 0.6 pmol of 5′-$^{32}$P-labeled target HIV-Loop. The mixture was heated at 90° for 3 min, cooled, and then the third strand was added so as to obtain the desired final concentration (10 μM in standard experiments). Glycerol with Bromophenol Blue and xylene cyanol (up to 5% of glycerol concentration) was then added, and the mixture was incubated for 5–16 h at 10°. The samples were loaded onto 12% nondenaturing polyacrylamide gel. Electrophoresis was performed in a cold box (10–13°) at a power not exceeding 6 W. To test the stability of the triplexes at higher pH, the following buffers were used: 50 mM *HEPES* (pH 7.5) or 89 mM *TBE* (pH 8.3), with 50 mM NaCl, and 5 mM $MgCl_2$ solns. The thermal stabilities of triple complexes were determined at 37, 45, 55, or 65° by gel-shift assays at pH 6.0.

*Determination of Triple-Helix Apparent Dissociation Constants.* Triple-helix dissociation constants $K_d$ were determined *via* gel-shift assay (pH 6.0, $T = 10°$) at different concentrations of the third strand: 10, 50, 100, 200, and 500 nM. The dissociation constants were obtained from *Eqn. 1* (excess of the third strand with respect to the duplex).

$$\lg C_0 = \lg K_D + \lg\left(\frac{x}{1-x}\right) \quad (1)$$

Here, $C_0$ is the initial concentration of the triplex-forming component, $K_d$ is the dissociation constant, and $x$ is the fraction of the duplex involved in triple-helix formation. The $K_d$ values were obtained from the y-intersection of the linear-regression curve of lg $C_0$ *vs.* lg ($x$/1 – x).

*Determination of Triple-Helix Apparent Association and Dissociation Rate Constants.* Kinetic experiments were performed by the gel-shift assay (pH 6.0, $T = 10°$), as described above, but without overnight incubation. The mixture of the target and the third strand was loaded onto the gel immediately after fixed incubation time intervals (0, 15, 30, 60, 120, and 180 min) with the third strand, assuming the following equilibrium: Duplex + TFO $\leftrightarrow$ Triplex, with $k_1$ and $k_{-1}$ being the triple-helix apparent association and dissociation rate constants, resp. This gives rise to *Eqn. 2*, where $k_{eff} = k_1 C_0$, $C_0$ being the initial concentration of TFO.

$$x(t) = \frac{k_{eff} \times (1 - e^{-(k_{eff}+k_{-1})t})}{k_{eff} + k_{-1}} \quad (2)$$

The rate constant $k_1$ were determined from *Eqn. 2*, using the experimentally determined values of $x$ as a function of time $t$, $x(t)$ being that part of the dsDNA that is involved in the triple-helix structure. The resulting data were analyzed with the SigmaPlot software (version 6.0).

## REFERENCES


[1] A. S. Boutorine, P. B. Arimondo, in 'Artificial Nucleases', Ed. M. A. Zenkova, Springer, Berlin, Heidelberg, 2004, p. 243.
[2] C. Malvy, L. L. Pritchard, A. Harel-Bellan, 'Triple Helix Forming Oligonucleotides', Kluwer Academic Publishers, Boston, 1999.
[3] J. M. Gottesfeld, J. M. Turner, P. B. Dervan, *Gene Expr.* **2000**, *9*, 77.
[4] J. S. Sun, T. Garestier, C. Hélène, *Curr. Opin. Struct. Biol.* **1996**, *6*, 327.
[5] D. Praseuth, A. L. Guieysse, C. Hélène, *Biochim. Biophys. Acta – Gene Struct. Express.* **1999**, *1489*, 181.
[6] C. Giovannangeli, C. Hélène, *Curr. Opin. Mol. Ther.* **2000**, *2*, 288.
[7] P. B. Dervan, R. W. Bürli, *Curr. Opin. Chem. Biol.* **1999**, *3*, 688.
[8] P. B. Dervan, *Bioorg. Med. Chem.* **2001**, *9*, 2215.
[9] M. E. Parks, E. E. Baird, P. B. Dervan, *J. Am. Chem. Soc.* **1996**, *118*, 6153.
[10] J. M. Turner, E. E. Baird, P. B. Dervan, *J. Am. Chem. Soc.* **1997**, *119*, 7636.
[11] J. W. Trauger, E. E. Baird, P. B. Dervan, *J. Am. Chem. Soc.* **1998**, *120*, 3534.
[12] M. A. Marques, R. M. Doss, S. Foister, P. B. Dervan, *J. Am. Chem. Soc.* **2004**, *126*, 10339.
[13] P. E. Floreancig, S. E. Swalley, J. W. Trauger, P. B. Dervan, *J. Am. Chem. Soc.* **2000**, *122*, 6342.
[14] F. P. Svinarchuk, J. R. Bertrand, C. Malvy, *Nucl. Acids Res.* **1994**, *22*, 3742.
[15] F. P. Svinarchuk, J. Paoletti, C. Malvy, *J. Biol. Chem.* **1995**, *270*, 14068.
[16] J. W. Szewczyk, E. E. Baird, P. B. Dervan, *Angew. Chem., Int. Ed.* **1996**, *35*, 1487.
[17] A. N. Sinyakov, V. A. Ryabinin, G. N. Grimm, A. S. Boutorine, *Mol. Biol. Engl. Trans.* **2001**, *35*, 251.
[18] Z. V. Zhilina, A. J. Ziemba, J. O. Trent, M. W. Reed, V. Gorn, Q. Zhou, W. Duan, L. Hurley, S. W. Ebbinghaus, *Bioconjugate Chem.* **2004**, *15*, 1182.
[19] C. R. Woods, T. Ishii, D. L. Boger, *J. Am. Chem. Soc.* **2002**, *124*, 10676.
[20] V. A. Ryabinin, A. S. Boutorine, C. Hélène, A. Y. Denisov, D. V. Pyshnyi, A. N. Sinyakov, *Nucleosides Nucleotides Nucleic Acids* **2004**, *23*, 953.
[21] V. A. Ryabinin, A. S. Boutorine, C. Hélène, D. V. Pyshnyi, A. N. Sinyakov, *Nucleosides Nucleotides Nucleic Acids* **2004**, *23*, 789.
[22] A. S.Boutorine, V. A. Ryabinin, D. S. Novopashina, A. G. Venyaminova, C. Hélène, A. N. Sinyakov, *Nucleosides Nucleotides Nucleic Acids* **2003**, *22*, 1267.
[23] C. Giovannangeli, S. Diviacco, V. Labrousse, S. Gryaznov, P. Charneau, C. Hélène, *Proc. Natl. Acad. Sci. U.S.A.* **1997**, *94*, 79.
[24] C. Escudé, J. S. Sun, M. Rougée, T. Garestier, C. Hélène, *C. R. Acad. Sci. Paris, Sci. de la Vie* **1992**, *315*, 521.
[25] M. Shimizu, A. Konishi, Y. Shimada, H. Inoue, E. Ohtsuka, *FEBS Lett.* **1992**, *302*, 155.
[26] M. Beban, P. S. Miller, *Biochim. Biophys. Acta, Gene Struct. Express.* **2000**, *1492*, 155.
[27] R. A. Cassidy, N. Puri, P. S. Miller, *Nucleic Acids Res.* **2003**, *31*, 4099.
[28] A. S. Boutorine, A. G. Venyaminova, M. N. Repkova, Z. A. Sergueyeva, D. V. Pyshnyi, *Biochimie* **1994**, *76*, 23.
[29] D. Novopashina, M. Kuznetsova, A. Venyaminova, *Nucleosides Nucleotides Nucleic Acids* **2001**, *20*, 903.
[30] Z. A. Kosolapova, A. G. Venyaminova, M. N. Repkova, *Bioorg. Khim.* **1990**, *16*, 635.
[31] G. N. Grimm, A. S. Boutorine, P. Lincoln, B. Nordén, C. Hélène, *ChemBioChem* **2002**, *3*, 324.

[32] M. Rougée, B. Faucon, J. L. Mergny, F. Barcelo, C. Giovannangeli, T. Garestier, C. Hélène, *Biochemistry* **1992**, *31*, 9269.
[33] Y. W. Park, K. J. Breslauer, *Proc. Natl. Acad. Sci. U.S.A.* **1992**, *89*, 6653.
[34] S. V. S. Mariappan, X. Cheng, R. B. van Breemen, L. A. Silks, G. Gupta, *Anal. Biochem.* **2004**, *334*, 216.
[35] V. Zarytova, E. Ivanova, A. Venyaminova, *Nucleosides Nucleotides* **1998**, *17*, 649.
[36] G. N. Grimm, A. S. Boutorine, C. Hélène, *Nucleosides Nucleotides Nucleic Acids* **2000**, *19*, 1943.
[37] E. Kostenko, M. Dobrikov, D. Pyshnyi, V. Petyuk, N. Komarova, V. Vlassov, M. Zenkova, *Nucleic Acids Res.* **2001**, *29*, 3611.
[38] Z. A. Sergeyeva, S. G. Lokhov, A. G. Venyaminova, *Bioorg. Khim.* **1996**, *22*, 916 (*Russ. J. Bioorg. Chem.* **1996**, *22*, 800).
[39] J. F. Ramalho-Ortigão, H. Rösch, H. Selter, A. Fröhlich, A. Lorenz, M. Montenarh, H. Seliger, *Antisense Res. Dev.* **1992**, *2*, 129.
[40] V. A. Efimov, A. A. Buryakova, S. V. Reverdatto, O. G. Chakhmakhcheva, *Bioorg. Khim.* **1983**, *9*, 1367.
[41] T. Horn, M. S. Urdea, *Tetrahedron Lett.* **1986**, *27*, 4705.
[42] P. J. Garegg, I. Lindh, T. Regberg, J. Stawinski, R. Stromberg, *Chem. Scripta* **1986**, *26*, 59.
[43] O. N. Koroleva, E. M. Volkova, V. L. Drutsa, *Bioorg. Khim.* **1994**, *20*, 420.
[44] V. A. Ryabinin, Y. A. Gorbunov, A. N. Sinyakov, *Bioorg. Khim.* **1997**, *23*, 539 (*Russ. J. Bioorg. Chem.* **1997**, *23*, 498).
[45] V. A. Ryabinin, A. N. Sinyakov, *Bioorg. Khim.* **1998**, *24*, 601 (*Russ. J. Bioorg. Chem.* **1998**, *24*, 531).
[46] A. Y. Denisov, V. A. Ryabinin, D. V. Pyshnyi, T. V. Abramova, A. N. Sinyakov, *Zhurn. Strukt. Khim*. **2001**, *42*, 111.
[47] A. N. Sinyakov, V. A. Ryabinin, S. V. Seregin, S. G. Lokhov, I. V. Kutyavin, H. B. Gamper, R. B. Mayer, *Bioorg. Khim*. **1997**, *23*, 544 (*Russ. J. Bioorg. Chem.* **1997**, *23*, 502).

*Received March 18, 2005*